Available online at www.sciencedirect.com
ScienceDirect
Biochimica et Biophysica Acta 1778 (2008) 466–471
Biochimica et Biophysica Acta
BBA
www.elsevier.com/locate/bbamem

Docosahexaenoic acid alters the size and distribution of cell surface microdomains

Robert S. Chapkin [a,b,*], Naisyin Wang [a,c], Yang-Yi Fan [b], Joanne R. Lupton [a,b], Ian A. Prior [d]

[a] Center for Environmental and Rural Health, Texas A&M University, College Station, Texas, USA
[b] Faculty of Nutrition, Texas A&M University, College Station, Texas, USA
[c] Department of Statistics, Texas A&M University, College Station, Texas, USA
[d] The Physiological Laboratory, University of Liverpool, Liverpool, United Kingdom

Received 1 June 2007; received in revised form 31 October 2007; accepted 7 November 2007
Available online 17 November 2007

Abstract

We recently generated nutritional data suggesting that chemoprotective dietary n-3 polyunsaturated fatty acids (n-3 PUFA) are capable of displacing acylated proteins from lipid raft microdomains *in vivo* [D.W. Ma, J. Seo, L.A. Davidson, E.S. Callaway, Y.Y. Fan, J.R. Lupton, R.S. Chapkin, n-3 PUFA alter caveolae lipid composition and resident protein localization in mouse colon, FASEB J. 18 (2004) 1040–1042; Y.Y. Fan, L.H. Ly, R. Barhoumi, D.N. McMurray, R.S. Chapkin, Dietary docosahexaenoic acid suppresses T cell protein kinase Cθ lipid raft recruitment and IL-2 recruitment, J. Immunol. 173 (2004) 6151–6160]. A primary source of very long chain n-3 PUFA in the diet is derived from fish enriched with docosahexaenoic acid (DHA, 22:6n-3). In this study, we sought to determine the effect of DHA on cell surface microdomain organization *in situ*. Using immuno-gold electron microscopy of plasma membrane sheets coupled with spatial point analysis of validated microdomain markers, morphologically featureless microdomains were visualized in HeLa cells at high resolution. Clustering of probes within cholesterol-dependent (GFP-tH) versus cholesterol-independent (GFP-tK) nanoclusters was differentially sensitive to n-3 PUFA treatment of cells. Univariate K-function analysis of GFP-tH (5 nm gold) revealed a significant increase in clustering ($p<0.05$) by pre-treatment with DHA and linoleic acid (LA, 18:$2^{\Delta 9,12}$) compared to control fatty acids; whereas LA significantly ($p<0.05$) reduced GFP-tK clustering. These novel data suggest that the plasma membrane organization of inner leaflets is fundamentally altered by PUFA-enrichment. We speculate that our findings may help define a new paradigm to better understand the complexity of n-3 PUFA modulation of signaling networks.

Keywords: Dynamic domain; Nanocluster; Omega-3 fatty acid; Microdomain

The plasma membrane of all eukaryotic cells is believed to consist of a mosaic of functional microdomains that facilitate interactions between resident proteins and lipids [1]. Visible examples of these include the early endocytic intermediates: clathrin-coated pits; and caveolae, flask shaped invaginations containing the structural protein caveolin-1 and many signal transduction proteins [2]. A morphologically featureless microdomain, consisting mostly of cholesterol and sphingolipids and therefore unable to integrate well into the fluid phospholipid bilayers was proposed by the lipid raft hypothesis [3]. Whilst evidence for the existence of lipid rafts has provoked debate, new sophisticated imaging approaches have started to define cell surface nanoscale organization [4,5]. Significantly, both cholesterol-dependent microdomains, analogous to lipid rafts, and non-raft signaling microdomains have been observed using electron microscopic imaging of 2D plasma membrane sheets [6]. These studies have provided a template for further investigation of cell surface organization and potential regulatory factors such as diet and disease.

With respect to the diverse biological effects of n-3 polyunsaturated fatty acids (PUFA), increasing evidence suggests that docosahexaenoic acid (DHA, 22:$6^{\Delta 4,7,10,13,16,19}$) is a unique fatty acid because it significantly alters basic properties of cell membranes, including acyl chain order and fluidity, phase behavior,

* Corresponding author. Department of Nutrition and Food Science, Center for Environmental and Rural Health, Kleberg Biotechnology Center, MS 2253, Texas A&M University, College Station, Texas 77843-2253, USA. Tel.: +1 979 845 0448; fax: +1 979 862 2378.
E-mail address: r-chapkin@tamu.edu (R.S. Chapkin).

0005-2736/$ - see front matter © 2007 Elsevier B.V. All rights reserved.
doi:10.1016/j.bbamem.2007.11.003

elastic compressibility, ion permeability, fusion, rapid flip-flop and resident protein function [7,8]. Because of its polyunsaturation, DHA is sterically incompatible with sphingolipid and cholesterol and, therefore, appears to alter lipid raft behavior [9]. Interestingly, a number of studies have recently demonstrated that dietary n-3 PUFA are incorporated into diverse cell types [10–12], and appear to uniquely modulate cell membrane microdomains [12–16]. Overall, these findings provide evidence indicating that dietary sources of n-3 PUFA can profoundly alter the biochemical make up of cell membrane lipid rafts/caveolae microdomains, which may directly or indirectly influence cell signaling, membrane fusion and protein trafficking [13,14,17,18].

In this study, we proposed that the aversion of DHA and possibly LA for cholesterol would increase the segregation of cholesterol into lipid rafts, thereby enhancing the extent of proteins clustering within lipid rafts. We investigated our hypothesis by utilizing immuno-gold electron microscopy of plasma membrane sheets coupled with spatial point analysis of marker proteins for cell surface microdomains in order to determine the influential role of different fatty acids.

1. Materials and methods

1.1. Reagents

Expression vectors for GFP-tagged truncated forms of H-Ras and K-Ras, GFP-tH, and GFP-tK were utilized as previously described [19,20]. 5 nm gold-conjugated anti-GFP antibodies were prepared by tannic acid/citrate method [6].

1.2. Electron microscopy and image analysis

HeLa cells (80–90% confluent) were maintained in DMEM supplemented with 5% fetal calf serum (Invitrogen) at 37 °C. Fatty acid treatment with 50 μM bovine serum albumin-bound oleic acid (OA: $18{:}1^{\Delta 9}$), linoleic acid (LA: $18{:}2^{\Delta 9,12}$), or DHA was initiated 48 h prior to transfection and was continued until cells were examined 36–48 h post-transfection. Medium containing 50 μM BSA-lipids was replaced every 24 h, and 12–16 h pre-transfection cells were split onto coverslips (40–50% confluency). Transient transfection was performed using GeneJuice (Novagen) according to the manufacturers' instructions; 5 h post-transfection the medium was replaced with fresh fatty acid-supplemented medium. All transfection conditions were optimized to minimize the amounts of DNA and lipofection reagent and the length of incubation time in order to reduce any nonspecific cytotoxicity.

Immuno-gold electron microscopy of cytoplasmic face-up plasma membrane sheets coupled with spatial point analysis of lipid rafts was performed as we have previously described [6,19,20]. Briefly, following transfection and lipid treatment, cells on coverslips were pressed onto coated grids, separated to generate plasma membrane sheets (inner leaflet face-up) and fixed with 4% PFA, 0.1% glutaraldehyde. Following labeling with 5 nm gold-conjugated anti-GFP, membrane sheets were digitally imaged using an FEI Tecnai G^2 120 kV transmission electron microscope. Images were recorded at 100,000×, 10–20 images per sample, and 0.8 μm^2 areas of digitized negatives were processed using Image J (http://rsb.info.nih.gov/ij/) to identify gold pattern co-ordinates for subsequent statistical analysis. Three independent experiments were performed with each treatment in each experiment consisting of 8–16 lawns analyzed. Mean gold densities per treatment dataset varied from 90–250 gold/μm^2.

1.3. Statistics

Ripley's K-function was used to discriminate patterns showing (i) dispersed, (ii) large clusters, (iii) small clusters, and (iv) mixed large clusters and dispersed. Values of $L(r) - r$ above the 99% confidence interval (normalized to 1.0) indicates significant clustering within the defined radius (r), below −1.0 indicates significant dispersal [19]. To compare the clustering patterns between treatments, we performed inferences by bootstrapping and Monte Carlo procedures. This approach is equivalent to generating 500 sets of new data according to distributions in the original data set, followed by performing inferences using the resulting 500 differences between two mean $L(r)$ functions. This procedure takes into account the between-process and the within-process variation. To account for the between-process variation, we sampled with replacement among the $L(r)$ functions from each treatment group. When a function was sampled, a spatial

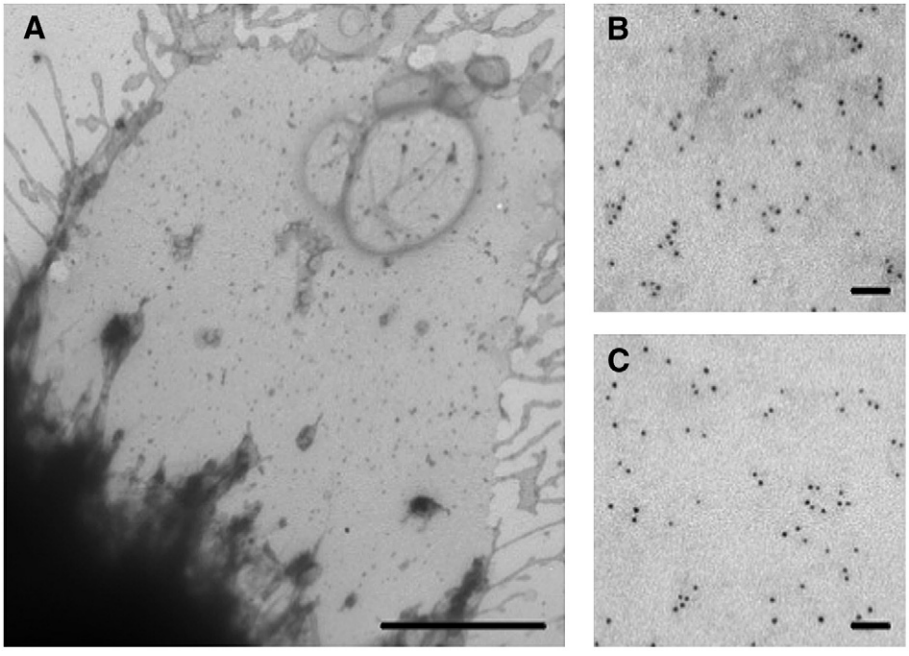

Fig. 1. Electron microscopy imaging of microdomains within 2D plasma membrane sheets. (A) Rip-offs have smooth homogenous shading compared to grainy background of grid. Bar = 1 μm. Representative electron micrograph image of immuno-gold labeled GFP-tH (B) and GFP-tK (C), bars = 50 nm.

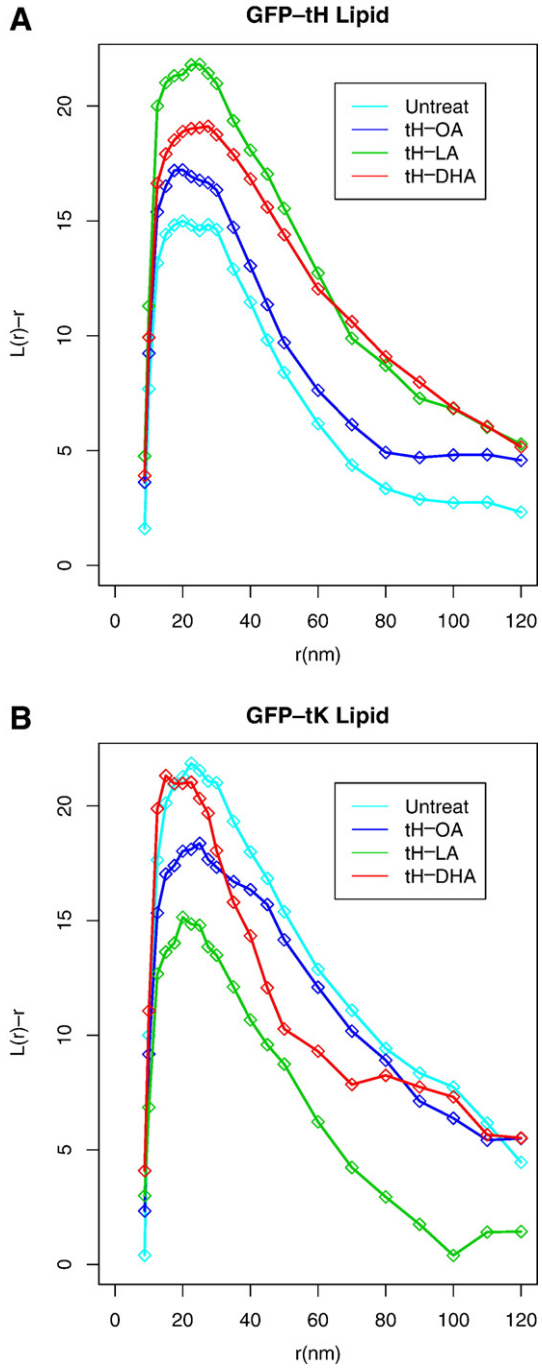

Fig. 2. Analysis of inner leaflet raft (tH) and non-raft (tK) markers. Ripley's K-function analysis of immuno-gold co-ordinates enables the extent of clustering within a 2D point pattern to be determined. Positive deflection from $L(r)-r=0$ indicates a tendency for clustering. All cultures were treated with OA, LA or DHA (50 μM) for 96 h, UT-untreated. Top panel (A), GFP-truncated H-ras (located exclusively to inner leaflet rafts); displays an increase in clustering with LA and DHA pre-treatment. Bottom panel (B), GFP-truncated K-ras (non-raft marker) exhibits a small decrease in cluster size (DHA) or total clustering (LA and UT). K-functions (8–16 lawns) are means ($n>500$ particles) from 3 separate experiments.

point process was re-generated according to an intensity function that was estimated non-parametrically using the data from the original point process [21,22,23]. An $L(r)$ function and its deviation from the mean were calculated and this deviation was added to the original function to create a new $L(r)$ function. This data-regenerating procedure accounts for the within-process variation. The point-by-point averages of the $L(r)$ functions were calculated for each treatment group and pairwise differences between each two treatments were obtained. The procedure was repeated 500 times and confidence intervals for treatment differences were constructed. Two treatments were considered to have different clustering patterns when any part of the zero line was outside the corresponding confidence interval.

2. Results and discussion

A combined immuno-electron microscopy–statistical approach was used to directly visualize morphologically featureless plasma membrane microdomains. Plasma membrane sheets from HeLa cells were typically found at the margins of cells and characterized by their smooth homogeneous shading compared to the grainy background of the grid (Fig. 1A). Immuno-gold labeling of validated raft (GFP-truncated H-ras; GFP-tH) and non-raft/disordered (GFP-truncated K-ras; GFP-tK) microdomain markers appeared indistinguishable (Fig. 1B and C). However, statistical analysis of plasma membrane sheets revealed differences in the extent of clustering tendency and size of gold-labeled clusters (Fig. 2). GFP-tH is targeted by a combination of palmitoylation and a farnesylated CAAX motif to lipid rafts [6,24]. K-function analysis of GFP-tH sheets revealed that the gold pattern was clustered, i.e., the curves exhibited a significant positive deviation from the $L(r)-r=0$ value expected for a random point pattern (data not shown). Interestingly, both DHA and LA treatments enhanced ($p<0.05$) the curve peak heights, i.e. exhibited increased clustering of the lipid raft probe, as compared to OA and untreated cells (Figs. 2 and 3). In contrast, analysis of GFP-tK labeled gold patterns revealed clustering, but with different characteristics relative to GFP-tH (Figs. 2 and 4). Whilst superficially both LA and OA decreased total GFP-tK clustering (Fig. 2), pairwise analysis of GFP-tK K-functions revealed that only LA treatment significantly ($p<0.05$) reduced clustering in non-raft regions of plasma membranes (Fig. 4). Interestingly, the DHA-induced shift to the left of the curve for GFP-tK compared to untreated control indicates that non-raft cluster sizes also appear to be decreased in the presence of this lipid (Fig. 2). Collectively, these data suggest that the plasma membrane organization of inner leaflets is fundamentally altered by polyunsaturated fatty acids. Specifically, PUFA increase clustering of proteins in cholesterol-dependent microdomains (GFP-tH), whereas non-raft microdomains are insensitive to n-3 PUFA modulation.

It is now appreciated that dietary PUFA are incorporated into both cholesterol/sphingolipid-rich detergent-resistant liquid ordered (l_o) and liquid disordered (l_d) plasma membrane microdomains in many cell types [11–15]. For example, DHA is enriched 2–3 folds in both raft (0.6 to 5.3 mol%) and non-raft (2.4 to 7.6 mol%) domains following incorporation into the diet [11–13]. The poor affinity of DHA and perhaps other long chain PUFA for cholesterol provides a lipid-driven mechanism for lateral phase separation of cholesterol/sphingolipid-rich lipid microdomains from the surrounding l_d phase in model membranes [7,9]. This could alter the size, stability and distribution of cell surface lipid microdomains such as rafts. Indeed, it has been proposed that microdomain enrichment of PUFA may alter the dynamic partitioning of acylated proteins,

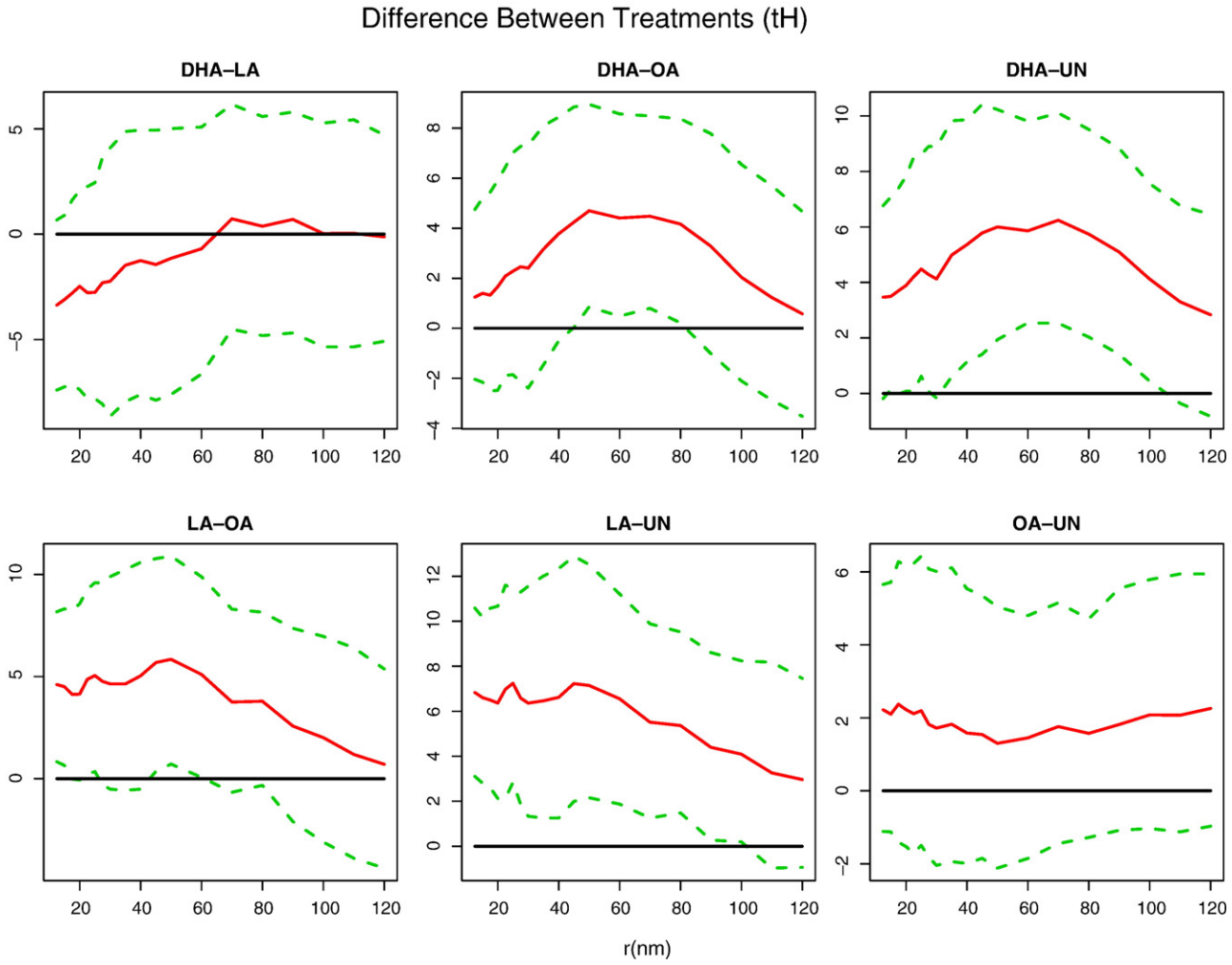

Fig. 3. Difference between inner leaflet raft (tH) treatments: pairwise comparison plots. The red solid line is the mean difference between two L(r) functions; the dashed green lines mark the 95% confidence interval. There exists a statistically significant difference between the two L(r) functions at the 0.05 level ($p<0.05$) when part of the solid black zero line is outside the two dashed green curves. X-axis indicates the radius r (nm) in which the L(r) function is calculated. Y-axis indicates the difference between the two L(r) functions.

thereby disrupting signal transduction events required for cell proliferation, apoptosis and differentiation [9,13,14,25,26]. However, the ability of DHA and other fatty acids to influence lateral organization of lipid raft microdomains *in situ* has not been determined to date. Experimental outcomes regarding biochemical isolation of microdomains vary depending on the isolation method, choice of detergent and cell type [5,27]. To circumvent some of the problems associated with these we chose to utilize a more direct electron microscopic statistical approach in order to generate 2D spatial maps with nanometer scale resolution of inner leaflet cell surface microdomains. In general, electron microscopy reveals a more complex and dynamic topographical organization of membrane microdomains than is predicted by biochemical analysis of detergent-resistant membranes [28,29]. In a major step toward developing a unifying mechanistic hypothesis addressing how dietary PUFA modulate cell membrane microdomains, we demonstrate for the first time that DHA and LA differentially affect inner leaflet rafts and non-raft membrane microdomains. These findings highlight a novel modality by which PUFA influence membrane micro-organization.

In conclusion, we have shown for the first time that DHA and LA, major dietary fatty acids, differentially modulate inner leaflet cholesterol-dependent versus cholesterol-independent membrane microdomains. This is significant because the health benefits of select fatty acids are diverse and nutritional studies continue to demonstrate important benefits from the consumption of n-3 PUFA-enriched oils. Recently, the U.S. Food and Drug Administration (FDA) has approved the use of a health claim on labels for foods containing n-3 PUFA. Therefore, it is both appropriate and timely to precisely determine how DHA and other fatty acids modulate cell membrane structure/function.

Acknowledgements

Supported in part by a University Research Fellowship from the Royal Society (IAP) and NIH grants CA59034 (RSC),

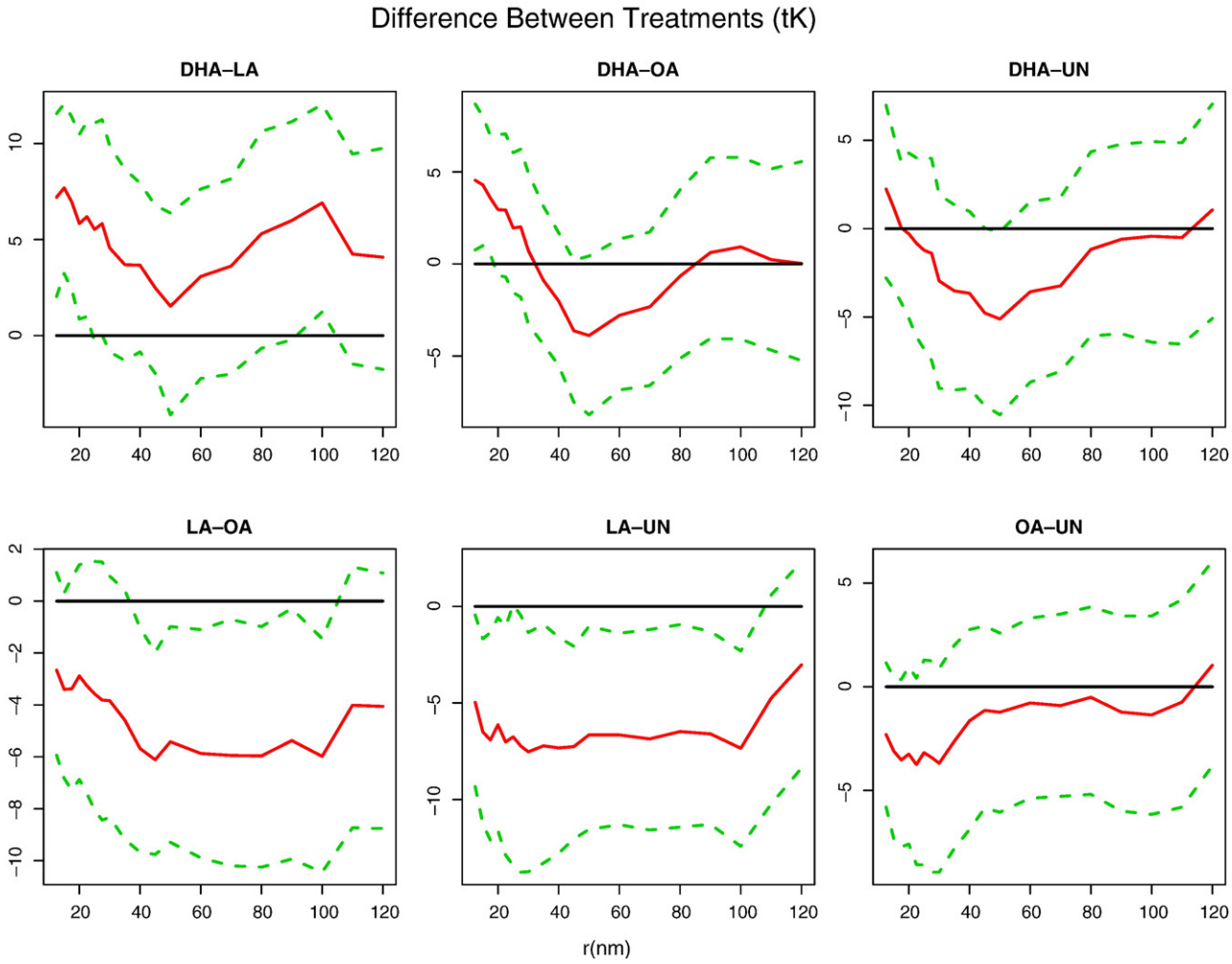

Fig. 4. Difference between inner leaflet non-raft (tK) treatments: pairwise comparison plots. Refer to Fig. 3 for legend details.

CA129444 (RSC), DK71707 (RSC), CA74552 (NW) and P30ES09106.

References

[1] A.J. Laude, I.A. Prior, Plasma membrane microdomains: organization, function and trafficking, Mol. Membr. Biol. 21 (2004) 193–205.
[2] R.G.W. Anderson, The caveolae membrane system, Annu. Rev. Biochem. 67 (1998) 199–225.
[3] K. Simons, E. Ikonen, Functional rafts in cell membranes, Nature 387 (1997) 569–572.
[4] S. Munro, Lipid rafts: elusive or illusive? Cell 115 (2003) 377–388.
[5] J.F. Hancock, Lipid rafts: contentious only from simplistic standpoints, Nat. Rev., Mol. Cell Biol. 7 (2006) 456–462.
[6] I.A. Prior, C. Muncke, R.G. Parton, J.F. Hancock, Direct visualization of Ras proteins in spatially distinct cell surface microdomains, J. Cell Biol. 160 (2003) 165–170.
[7] W. Stillwell, S.R. Wassall, Docosahexaenoic acid: membrane properties of a unique fatty acid, Chem. Phys. Lipids 126 (2003) 1–27.
[8] S.R. Shaikh, M. Caffrey, W. Stillwell, V. Cherezov, S.R. Wassall, Interaction of cholesterol with docosahexaenoic acid-containing phosphatidylethanolamine: trigger for microdomain/raft formation? Biochemistry 42 (2003) 12028–12037.
[9] S.R. Shaikh, A.C. Dumaual, A. Castillo, D. LoCascio, R.A. Siddiqui, W. Stillwell, S.R. Wassall, Oleic and docosahexaenoic acid differentially phase separate from lipid raft molecules: a comparative NMR, DSC, AFM, and detergent extraction study, Biophys. J. 87 (2004) 1752–1766.
[10] M.Y. Hong, R.S. Chapkin, R. Barhoumi, R.C. Burghardt, N.D. Turner, C.E. Henderson, L.M. Sanders, Y.Y. Fan, L.A. Davidson, M.E. Murphy, C.M. Spinka, R.J. Carroll, J.R. Lupton, Fish oil increases mitochondrial phospholipid unsaturation, upregulating reactive oxygen species and apoptosis in rat coloncytes, Carcinogenesis 23 (2002) 1919–1925.
[11] Y.Y. Fan, D.N. McMurray, L.H. Ly, R.S. Chapkin, Dietary (n-3) polyunsaturated fatty acids remodel mouse T-cell lipid rafts, J. Nutr. 133 (2003) 1913–1920.
[12] Y.Y. Fan, L.H. Ly, R. Barhoumi, D.N. McMurray, R.S. Chapkin, Dietary docosahexaenoic acid suppresses T cell protein kinase Cθ lipid raft recruitment and IL-2 recruitment, J. Immunol. 173 (2004) 6151–6160.
[13] D.W. Ma, J. Seo, L.A. Davidson, E.S. Callaway, Y.Y. Fan, J.R. Lupton, R.S. Chapkin, n-3 PUFA alter caveolae lipid composition and resident protein localization in mouse colon, FASEB J. 18 (2004) 1040–1042.
[14] D.W. Ma, J. Seo, K.C. Switzer, Y.Y. Fan, D.N. McMurray, J.R. Lupton, R.S. Chapkin, n-3 PUFA and membrane microdomains: a new frontier in bioactive lipid research, J. Nutr. Biochem 15 (2004) 700–706.
[15] M. Zeyda, M.D. Saemann, K.M. Stuhlmeir, D.G. Mascher, P.N. Nowotny, G.J. Zlabinger, W. Waldhausl, T.M. Stulnig, Polyunsaturated fatty acids block dendritic cell activation and function independently of NF-κB activation, J. Biol. Chem. 280 (2005) 14293–14301.
[16] R. Geyeregger, M. Zeyda, G.J. Zlabinger, W. Waldausl, T.M. Stulnig, Polyunsaturated fatty acids interfere with formation of the immunogical synapse, J. Leukoc. Biol. 77 (2005) 680–688.

[17] J. Seo, R. Barhoumi, A.E. Johnson, J.R. Lupton, R.S. Chapkin, Docosahexaenoic acid selectively inhibits plasma membrane targeting of lapidated proteins, FASEB J. 20 (2006) 770–772.
[18] F. Darios, B. Davletov, Omega-3 and omega-6 fatty acids stimulate cell membrane expansion by acting on syntaxin 3, Nature 440 (2006) 813–817.
[19] I.A. Prior, R.G. Parton, J.F. Hancock, Observing cell surface signaling domains using electron microscopy, Sci. STKE 177 (Apr 8 2003) PL9.
[20] J.F. Hancock, I.A. Prior, Electron microscopic imaging of Ras signaling domains, Methods 37 (2005) 165–172.
[21] P.J. Diggle, A kernel method for smoothing point process data, Appl. Stat. 34 (1985) 138–147.
[22] W.N. Venables, B.D. Ripley, Modern Applied Statistics with S, 4th Edition, Springer, 2002.
[23] P.J. Diggle, Statistical Analysis of Spatial Point Patterns, Academic Press, London, 1983.
[24] I.A. Prior, A. Harding, J. Yan, J. Sluimer, R.G. Parton, J.F. Hancock, GTP-dependent segregation of H-ras from lipid rafts is required for biological activity, Nat. Cell Biol. 3 (2001) 368–375.
[25] S.J. Plowman, C. Muncke, R.G. Parton, J.F. Hancock, H-ras, K-ras, and inner membrane raft proteins operate in nanoclusters with differential dependence on the actin cytoskeleton, Proc. Natl. Acad. Sci. 102 (2005) 15500–15505.
[26] R.S. Chapkin, D.N. McMurray, J.R. Lupton, Colon cancer, fatty acids and anti-inflammatory compounds, Curr. Opin. Gastroenterol. 23 (2007) 48–54.
[27] S. Schuck, M. Honsho, K. Ekroos, A. Shevchenko, K. Simons, Resistance of cell membranes to different detergents, Proc. Natl. Acad. Sci. 100 (2003) 5795–5800.
[28] B.S. Wilson, S.L. Steinberg, K. Liederman, J.R. Pfeiffer, Z. Suriladze, J. Zhang, L.E. Samelson, L. Yang, P.G. Kotula, J.M. Oliver, Markers for detergent-resistant lipid rafts occupy distinct and dynamic domains in native membranes, Mol. Biol. Cell 15 (2004) 2580–2592.
[29] J. Zhang, K. Leiderman, J.R. Pfeiffer, B.S. Wilson, J.M. Oliver, S.L. Steinberg, Characterizing the topography of membrane receptors and signaling molecules from spatial patterns obtained using nanometer-scale electron-dense probes and electron microscopy, Micron 37 (2006) 14–34.